Acta Biomaterialia 7 (2011) 67–74

Contents lists available at ScienceDirect

Acta Biomaterialia

journal homepage: www.elsevier.com/locate/actabiomat

Tuning adhesion failure strength for tissue-specific applications

Natalie Artzi [a,b,*], Adam Zeiger [c], Fiete Boehning [a], Adriana bon Ramos [a,d], Krystyn Van Vliet [c], Elazer R. Edelman [a,e]

[a] Harvard–MIT Division of Health Sciences and Technology, Massachusetts Institute of Technology, Cambridge, MA 02139, USA
[b] Anasthesiology Division, Brigham and Women's Hospital, Harvard Medical School, Boston, MA 02115, USA
[c] Materials Science and Engineering, Massachusetts Institute of Technology, Cambridge, MA 02139, USA
[d] Department of Chemistry, Institut Quimic de Sarria, Universitat Ramon Llull, Barcelona 08017, Spain
[e] Cardiovascular Division, Department of Medicine, Brigham and Women's Hospital, Harvard Medical School, Boston, MA 02115, USA

ARTICLE INFO

Article history:
Received 30 April 2010
Received in revised form 28 June 2010
Accepted 7 July 2010
Available online 23 July 2010

Keywords:
Adhesion
AFM
Biocompatibility
Mechanical properties
Tissue adhesive

ABSTRACT

Soft tissue adhesives are employed to repair and seal many different organs, which range in both tissue surface chemistry and mechanical challenges during organ function. This complexity motivates the development of tunable adhesive materials with high resistance to uniaxial or multiaxial loads dictated by a specific organ environment. Co-polymeric hydrogels comprising aminated star polyethylene glycol and dextran aldehyde (PEG:dextran) are materials exhibiting physico-chemical properties that can be modified to achieve this organ- and tissue-specific adhesion performance. Here we report that resistance to failure under specific loading conditions, as well as tissue response at the adhesive material–tissue interface, can be modulated through regulation of the number and density of adhesive aldehyde groups. We find that atomic force microscopy (AFM) can characterize the material aldehyde density available for tissue interaction, and in this way enable rapid, informed material choice. Further, the correlation between AFM quantification of nanoscale unbinding forces with macroscale measurements of adhesion strength by uniaxial tension or multiaxial burst pressure allows the design of materials with specific cohesion and adhesion strengths. However, failure strength alone does not predict optimal in vivo reactivity. Thus, we demonstrate that the development of adhesive materials is significantly enabled when experiments are integrated along length scales to consider organ chemistry and mechanical loading states concurrently with adhesive material properties and tissue response.

1. Introduction

Adhesive materials significantly expand the resources available for wound repair and surgical interventions [1–3]. Synthetic adhesives can enhance the support and augmentation of soft tissue organs such as the heart and intestine or hard tissues such as bone and teeth [4–6]. However, this wide array of target tissue applications provides a unique challenge, requiring adhesive materials that differ greatly in their physico-chemical properties to meet the varying demands of a wide range of tissue compositions and mechanical loading conditions. Commercially available adhesive sealants, such as fibrin glue and cyanoacrylates, often require a choice between degree of adhesion and biocompatibility [7–9]. Modification of the adhesive material composition or macromolecular chain architecture can modulate adhesion without pushing this balance towards toxicity. For example, the addition of biomimetic functional groups, such as L-3,4-dihydroxylphenylalanine (DOPA), can enhance the adhesion of materials to surfaces and tissues [10] through fully reversible, noncovalent interactions [11]. Alternatively, nanopatterned surfaces increase the contact surface area between the adhesive [12] and tissue. However, neither this general DOPA addition nor surface topographical roughening is specific to the morphology of the target tissue or the mechanical requirements of the target organ.

This issue of tissue responsiveness has taken on increased importance given the recently demonstrated capacity to modulate the extent of tissue interaction with synthetic adhesive polymers in a tissue-specific manner [13]. For example, we have shown that PEG:dextran aldehyde co-polymer materials bind differentially to lung, liver, heart or small intestine. This tissue-specific contrast is consistent with the concept that each tissue presents a different landscape of surface amines for interaction with adhesive material aldehydes. Thus, in such a material system, adhesion and biocompatibility are optimized through modulation of amine–aldehyde interactions [13]. As the field moves to the design and application of such materials with tissue-specific modulated adhesion, knowledge of the surface properties of both the target tissue and the

* Corresponding author at: Harvard–MIT Division of Health Sciences and Technology, Massachusetts Institute of Technology, Cambridge, MA 02139, USA. Tel.: +1 617 253 8146; fax: +1 617 253 2514.
E-mail address: nartzi@mit.edu (N. Artzi).

1742-7061/$ - see front matter © 2010 Acta Materialia Inc. Published by Elsevier Ltd. All rights reserved.
doi:10.1016/j.actbio.2010.07.008

adhesive becomes paramount. Further, the loading state of the adhesive in the tissue or organ of interest must be considered, to distinguish between potential adhesive and cohesive failure modes of the tissue–adhesive material seal.

The PEG:dextran family of materials provides a model system for examining chemically directed adhesion [13,14]. There exist at least six different parameters that can be varied to create materials with the full spectrum of adhesion, including: solid content and molecular weight of the two components; degree of aldehyde oxidation; number of arms in the stellate PEG [15]. A cross-linked network of PEG:dextran is formed via binding between aldehydes and amines. Those aldehydes that are still free remain reactive, such that adhesive bonds can form between this network and opposing amines of adjacent tissues. However, an excess of aldehydes can give rise to a toxic tissue response. Identification of design parameters that maximize adhesion while minimizing adverse tissue responses requires efficient materials characterization at complex interfaces.

In this study of PEG:dextran adhesives of variable compositions we demonstrate and correlate experimental approaches that can be used to quantify tissue–adhesive interactions relevant to the mechanical challenges of soft tissue adhesives in vivo. Atomic force microscopy (AFM)-mediated force spectroscopy can characterize the aldehyde density of such synthetic adhesive materials available for tissue interaction, and in this way enable rapid, informed material choice. Here, cantilevered AFM probes were functionalized with amines to mimic tissue surfaces and used to quantify interaction potential with a compositionally varied series of aldehyde-presenting adhesive gels. Adhesion strength between these characterized gels and a tissue comprising the small intestine was measured ex vivo at the macro scale. The macro scale failure loads and pressures correlated with the unbinding force measured via AFM force spectroscopy when aldehyde group numbers were varied (compositions A–C), but did not correlate when aldehyde density was altered (compositions A vs. D). As anticipated, maximal adhesion strength ex vivo did not necessarily correlate with optimized in vivo function: those adhesive gels exhibiting excess aldehyde groups resulted in increased inflammation of the small intestine in vivo. Thus, the development of adhesive materials will advance most rapidly when experiments are integrated to consider the chemistry and mechanical loading state of the target organ concurrently with adhesive properties and tissue response.

2. Materials and methods

2.1. Synthesis and formation of PEG:dextran

Star PEG amine, dextran aldehydes and PEG:dextran networks were fabricated as described previously [13,15]. Briefly, eight arm 10 kDa star PEG polymer with amine terminal groups was dissolved in water to give 10–50 wt.% solutions. Linear dextran (10 kDa) was oxidized with sodium periodate to create dextran aldehyde (50% oxidation of glucose rings, 2 aldehyde groups per oxidized glucose ring), which was also prepared as an aqueous solution (8.75–23 wt.%). The two homogeneous polymer solutions were loaded into a dual chamber syringe equipped with a 12 step mixing tip. The PEG:dextran network formation occurred within seconds to minutes, following the controlled mixing of PEG amine and dextran aldehyde via a Schiff base reaction between the constituent reactive groups (aldehydes and amines).

2.2. Selection and designation of PEG:dextran variants

Solid content, molecular weight and reactive group content of both PEG amine and dextran aldehyde polymers can be altered to create variable cross-linked networks and material properties. As the ratio of aldehyde to amine-reactive group concentrations, designated $CHO:NH_2$, is held constant the formulations under study are meaningfully differentiated by the total number of aldehydes. To evaluate the importance of aldehyde density on the resulting material performance, dextran oxidation level (hereafter, termed percent oxidation) was altered while keeping the total number of aldehydes constant (see Table 1).

2.3. Atomic force microscopy (AFM) spectroscopy of adhesive unbinding forces

AFM-enabled force spectroscopy was conducted to compare the unbinding force between PEG:dextran aldehyde-presenting materials and opposing amine-presenting surfaces. Silicon cantilevers terminating in colloidal silica spheres of nominal radius $R = 1$ μm (Nanosensors, Neuchatel, Switzerland) were cleaned by ozone treatment. Probes were then functionalized with amine groups by chemical vapor deposition using evaporation of 3-(aminopropyl)triethoxysilane (APTES) and N,N-diisopropylethylamine within a dessicator for 2 h.

Calibration of inverse optical lever sensitivity in terms of the photodiode voltage ($nm\,V^{-1}$) and cantilever spring constant k (nominally $0.1\,N\,m^{-1}$) were conducted as previously described [16]. Samples were immersed and fully hydrated in phosphate-buffered saline (PBS) upon polymerization. The acquired probe deflection–piezoactuator displacement responses during approach and retraction from the adhesive material surfaces were converted offline (Scanning Probe Imaging Processor, Image Metrology, Hørsholm, Denmark) to force–distance responses. Maximum loads and contact areas were 5 nN and 2.4 μm^2, respectively, in order to sample multi-molecular rather than single molecule interactions. Contact areas were calculated from the measured depth of indentation and the manufacturer measured radius of the AFM spherical probes (1 μm). The unbinding force (F_R) is defined herein as the force required to separate the amine-functionalized probe from the surface of the adhesive, and serves as an indicator of the number of free aldehyde groups [17,18] available for binding. The approach and separation velocities for all samples and replicate measurements was $6\,\mu m\,s^{-1}$, resulting in unloading rates that did not differ significantly among samples (ANOVA, $P < 0.05$). At least 30 replicate measurements were acquired per hydrated adhesive sample.

Table 1
Compositional description of the PEG:dextran compositions examined.

Composition		Dextran aldehyde			PEG amine			PEG:dextran
		Molecular weight (kDa)	Oxidation (%)	Solid content (%)	Arm number	Molecular weight (kDa)	Solid content (%)	Reactive group ratio ($CHO:NH_2$)
D10-50-8.75 P8-10-25	A	10	50	8.75	8	10	25	3
D10-50-14 P8-10-40	B	10	50	14	8	10	40	3
D10-50-18 P8-10-50	C	10	50	18	8	10	50	3
D10-20-23 P8-10-25	D	10	20	23	8	10	25	3

2.4. Macroscale interfacial adhesion strength and burst pressure measurements

Adult Sprague–Dawley rats (250–300 g, Charles River Laboratories, Shrewsbury, MA) were sacrificed by carbon dioxide asphyxiation under the university IACUC protocol and federal guidelines for animal care. Following sacrifice the duodenum (i.e. the first section of the small intestine) was excised and immersed in 10 ml of PBS (150 mM NaCl) at room temperature for macro scale characterization of adhesion strength and burst pressure. Selection of this animal model enabled the carrying out of the number of in vitro macro scale experiments required to establish the statistical significance of potential differences in tissue adhesion performance among the PEG:dextran materials.

To quantify the macro scale adhesion strength of explanted tissue each PEG:dextran adhesive gel was applied between two uniformly sized rat duodenal biopsies (8 mm diameter). After allowing polymerization at the tissue interfaces (5 min), monotonic uniaxial tensile testing (Biodynamic Test Instrument, Bose®, Minnetonka, MN) was employed at a constant rate (0.05 mm s^{-1}) and the load response was continuously recorded (200 measurements s^{-1}) to the point of macroscopic failure.

To quantify adhesive gel performance under mechanical loading related to small intestine function in vivo, longitudinal duodenal segments were cut and inserted into a mechanical testing apparatus configured for luminal perfusion (Bose® Biodynamic Test Instrument). The basis of this macroscopic test is the application of internal pressure to hollow organs or tissue sections, identifying failure in terms of the fluid pressure at which catastrophic mechanical failure occurs (i.e. burst pressure). A wound was introduced by puncturing the intestinal wall with an 18 gauge needle. Wounds were then repaired with a 200 μl application of PEG:dextran adhesive. After 5 min curing time, pulsatile loads were applied through perfusion with PBS. The burst pressure of repaired intestinal wounds was measured through a gradual increase in lumen pressure. A slow development of pressure was achieved through restriction of flow distal to the sample lumen and monitored at the inlet of the intestine. The burst pressure was easily detected, as failure of the repair site resulted in immediate loss of pressure and visible PBS leakage. The maximum luminal pressure prior to interface failure was recorded as the wound burst pressure.

2.5. Adhesive interface morphology

To investigate the morphology of the interface between the adhesives and the duodenal tissue the surface of biopsied longitudinal rat duodenal tissues was covered with fluorescently labeled PEG:dextran (fluorescein-conjugated PEG:dextran) and the material was allowed to cure for 10 min. Tissue samples were then cryosectioned (20 μm sections) and cell nuclei stained with DAPI (Vector Laboratories).

The morphology of the tissue–material interface was quantified as intensity of fluorescein at the interface using image analysis (MetaMorph®, Leica Microsystems).

2.6. In vivo biocompatibility

To investigate the effect of aldehyde content on tissue–material interaction and biocompatibility two material formulations containing 8.75 or 14 wt.% dextran aldehyde (D10-50-8.75 P8-10-25 or D10-50-14 P8-10-40) were applied to wounded small intestinal tissues of New Zealand rabbits and tissue response/repair was evaluated. This animal model has been demonstrated to be highly sensitive to tissue–material interactions of the duodenum, representing a more significant in vivo challenge than rat duodenum characterized in vitro. All experimental protocols were approved by the MIT Animal Care and Use Committee and were in compliance with NIH guidelines for animal use. Longitudinal cuts of 1 cm length were generated and 5-0 PDS II sutures were applied to close the wound. PEG:dextran sealants were applied on top of the sutures and allowed to cure for 5 min. Small intestinal tissues were harvested after 15 days, sectioned using a cryotome to produce 20 μm thick sections. Hematoxylin and eosin staining were performed using standard methods. Histopathological scoring via light microscopy was used to determine degree of inflammation, necrosis, hemorrhage, re-epithelialization, fibrosis and/or reactive fibrovascular proliferation, which reflect the extent of the host response/repair process to treatment with the bioadhesive. Scores of 0–3 were assigned to samples to indicate no, mild and notable or marked features present at the interface, respectively.

2.7. Statistical analysis

All macro scale data are presented as means ± standard deviation among samples, except for AFM measurements, which are presented as means ± standard error among replicate measurements on a single sample. Statistical analyses were performed using one-way ANOVA with Tukey analysis post tests. A P value <0.05 is considered statistically significant.

3. Results

Four PEG:dextran adhesive formulations were studied (Table 1). Compositions A–C consider variations in the relative number of free aldehyde groups. Compositions A and D provide a comparison of aldehyde group density (i.e. number of aldehyde groups per chain, via the extent of dextran oxidation), while attempting to maintain the overall number of free aldehyde groups per unit volume constant. Below we outline results characterizing the material, the in vitro tissue adhesion strength and failure and the in vivo biocompatibility as a function of these compositional variables.

3.1. AFM force spectroscopic analysis of unbinding force

We employed AFM-enabled force spectroscopy to compare unbinding forces among PEG:dextran material formulations, as a molecular scale screening tool for adhesion of these polymer adhesives to the amine-rich surfaces of tissues in vivo. AFM cantilevered probes functionalized with amine groups (Fig. 1A) were used to determine the unbinding force F_R between the tissue and PEG:dextran adhesive formulations. The micrometer scale probe amines interact exclusively with free aldehydes at the polymeric gel surfaces, and the unbinding force required to separate the amine-functionalized probe is therefore a measure of aldehyde binding potential. Note that this is not intended to be a single molecule level analysis of molecular unbinding, but rather provides a more controlled interface than tissues to explore the strength of multiple interactions on the micrometer scale. Variation in the relative number of free aldehyde groups (compositions A–C) significantly affected F_R (ranging from 0.31 ± 0.09 to 1.00 ± 0.25 nN, ANOVA $P < 0.001$), demonstrating the direct modulation of aldehyde-mediated adhesion efficiency via polymer design (Fig. 1B).

The effect of aldehyde group density imparted by changing the level of dextran aldehyde oxidation from 20% to 50% (compositions A and D) was less intuitive. Here, composition D presented a lower aldehyde density per chain, but the total number of aldehyde groups per unit volume was similar between these samples (Fig. 1B). In fact, the unbinding force required to rupture adhesion between the probe and these two adhesives was statistically distinguishable ($P < 0.05$). Given that these experiments proceeded

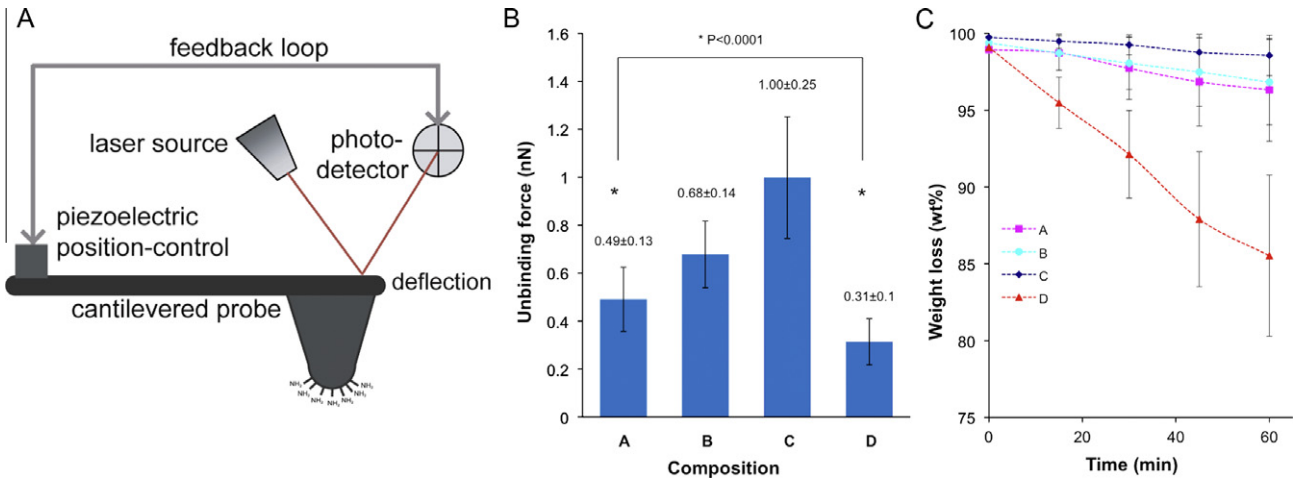

Fig. 1. (A) Schematic of AFM cantilevered probes functionalized with amine groups used to measure the rupture force between free amines and adhesive formulations, (B) rupture force for variation in the relative number of free aldehyde groups (compositions A–C, D10-50-8.75, D10-50-14 and D10-50-18 with P8-10-25) or aldehyde group density (composition D, D10-20-23 P8-10-25) and (C) degradation kinetics of the different adhesive formulations listed above. Values reported as averages ± standard error.

with the adhesives fully immersed and hydrated over the hour time scales required for data acquisition, we considered that polymer degradation proceeded differently for each sample and, therefore, the number of polymeric chains that interacted with available amine groups differed. To confirm this hypothesis, the degradation kinetics of the different adhesive formulations was assessed (Fig. 1C). 20% oxidation (composition D) resulted in a significantly accelerated degradation rate compared with 50% oxidation (composition A). This finding is consistent with the hypothesis that composition D, having a lower aldehyde group density per chain, formed a network less efficiently and, in turn, that less densely cross-linked networks were degraded more quickly upon immersion in aqueous solutions. In contrast, there was no statistically significant difference in degradation kinetics among samples A, B and C. Thus, these data illustrate both a limitation of AFM-based screening of the loss of adhesive forces and an advantage, in that such rapid degradation and loss of adhesion capacity makes clear that such a composition is ill-suited to most in vivo adhesive sealant applications.

3.2. Macroscale failure load under normal loading

A facile and most commonly reported method of comparing tissue adhesives is uniaxial tensile loading of macroscale tissue–adhesive–tissue constructs, in which load is applied normal to the adhesive interface [19,20]. Interfacial strength of the tissue–adhesive specimens (Fig. 2A and B) was assessed by applying a constant displacement rate (0.05 mm s^{-1}) normal to the tissue–adhesive–tissue interface (see Section 2). As the interfacial area is difficult to quantify, failure was quantified as the maximum applied tensile load (rather than applied stress). Here we observed that rupture of the tissue–adhesive–tissue structure occurred within the bulk of the adhesive for all tests, rather than at the tissue–adhesive interfaces. This finding demonstrates that these adhesives exhibited cohesive failure under this tensile mechanical loading mode. Although adhesive failure is the weakest link under this loading mode, the overall failure of the tissue–material–tissue construct is determined by both the material cohesive force and the adhesion strength at the tissue–material interface. If the adhesive unbinding force is higher as a function of solid content, the tissue–material–tissue construct failure load would be expected to show a similar trend even when the observed failure itself was cohesive. Hence, failure load for each composition (Fig. 2C) was compared with the molecular scale unbinding force (Fig. 1B). Indeed, a strong linear correlation ($R^2 = 0.973$) was observed. Thus, a concordance exists between molecular scale F_R and macro scale failure load of the adhesive materials cured on excised rat small intestinal tissue.

However, we note that for the most anticipated application of adhesives for small intestine repair the adhesive will be applied to an open wound on the tissue serosal layer and cured in vivo. The relevant loading state for such an application is better approximated by a measure of the burst pressure of the perfused organ. Next, we assessed interfacial strength through this macro scale method.

3.3. Burst pressure under internal loading

Excised intestinal tissues comprising a hollow lumen were wounded and repaired with each adhesive polymer composition (see Section 2). Following repair of a circular puncture wound, pulsatile loads were applied to the samples in a mechanical testing apparatus configured for luminal perfusion (Fig. 3A and B). Maximum luminal pressure prior to failure of the repair was recorded

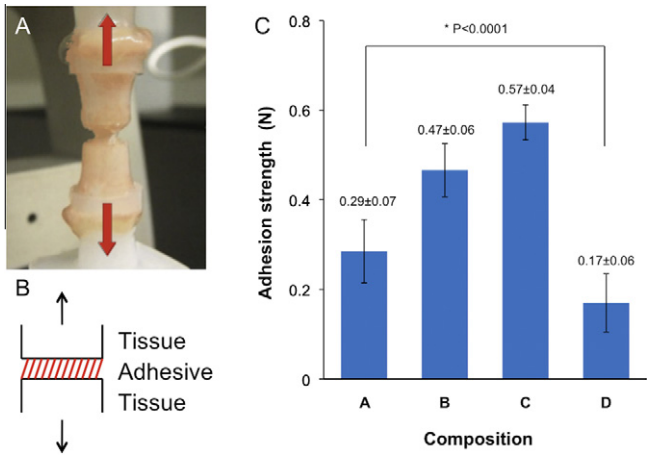

Fig. 2. (A) Image and (B) schematic of tissue–material–tissue interface in uniaxial tensile loading and (C) adhesion strength of compositions A–D applied to the rat small intestine. Values reported as averages ± standard deviation.

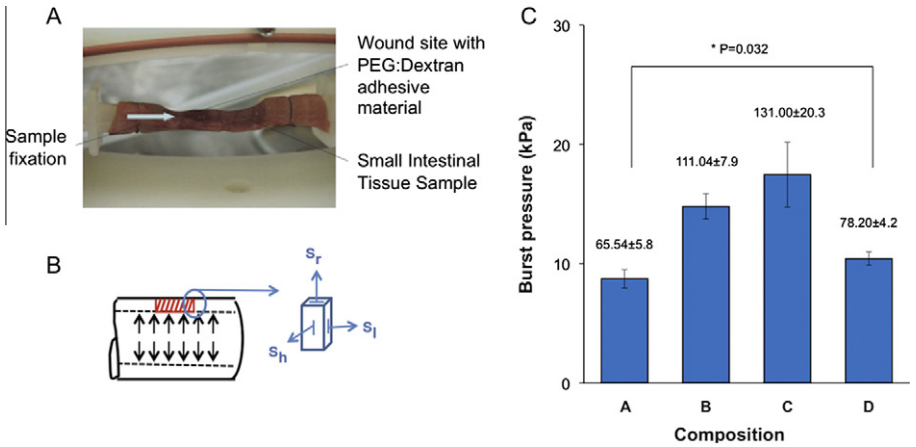

Fig. 3. (A) Image and (B) schematic of the burst pressure experiment. Stresses within and at the interface are multiaxial, including interfacial shear, as well as radial, longitudinal and hoop stresses σ_r, σ_l and σ_h. (C) Burst pressure of compositions A–D applied to the rat small intestine. Values reported as averages ± standard deviation.

as the burst pressure, indicating the adhesion strength under complex triaxial loading (Fig. 3C). Under these loading conditions a correlation between this burst pressure and macroscopic failure load was found for compositions A, B and C. However, the PEG:dextran adhesive formulation with 20% oxidation (composition D, 10.4 ± 0.53 kPa) demonstrated a significantly higher burst pressure compared with 50% oxidation (composition A, 8.7 ± 0.8 kPa, $P = 0.032$). Adhesive failure under triaxial loading was at the tissue–material interface. For reference, the maximal physiological pressures in the duodenum are typically 4 kPa [21], indicating that all compositions failed at super-physiological perfusion pressures.

In contrast to the cohesive failure modes observed under uniaxial tensile loading, adhesive failure was observed under burst pressure triaxial loading. In other words, failure of the seal always occurred directly at the tissue–material interface, as confirmed by the use of fluorescently labeled PEG in these PEG:dextran adhesives [13].

3.4. Ex vivo adhesive interface morphology

To elucidate the difference between compositions A and D, samples with the same total number of aldehyde groups that differed in oxidation level and thus aldehyde density per chain we examined the morphology of the interfacial region between these adhesives cured on excised rat small intestinal tissues (Fig. 4). Quantitative fluorescence microscopy indicated significant differences in the adhesive regimes. Three distinct domains were observed: the bulk adhesive, the tissue and the interface between them. Clear differences were observed in terms of (1) the width of this interface, (2) the size and number of pores, indicative of the extent of reaction with tissue amines and (3) the existence of a visible gap between the fluorescently labeled adhesive material and the tissue itself. Composition A exhibited a wider interfacial region, as well as a higher pore area ($W = 100.5 \pm 9.9$ μm and $\Phi = 476.7 \pm 100.9$ μm^2) compared with composition D ($W = 56.9 \pm 7.0$ μm and $\Phi = 150.6 \pm 15.2$ μm^2). There was also a visible gap in fluorescence intensity along all tissue interfaces. In contrast, composition D exhibited smaller and fewer pores within a narrower interfacial region, and no visible gap along a smoother interfacial line intersecting the tissue. This interface morphology demonstrates improved interfacial adhesion and integration of the material. Quantification of fluorescence intensity at the interfacial regime corroborated this increased integration of fluorescently labeled adhesive at the interface (relative intensities of 14.1 ± 1.2 and 19.3 ± 2.3 for compositions A and D, respectively). However, given the rapid degradation of composition D upon extended immersion (Fig. 2B), composition D is a suboptimal adhesive for the in vivo application of small intestine sealing. For final optimization of adhesive materials in vivo adhesion strength must be balanced against a minimal inflammatory response. Next, we consider this issue for the two materials in this array that exhibited differential adhesion strengths.

3.5. In vivo tissue interface pathology

The number of available aldehyde groups affects tissue biocompatibility, and can adversely offset the potential for strong tissue adhesion [13]. Here we evaluated the tissue response to compositions A and B, adhesives showing significantly different resistances to uniaxial and multiaxial loading, without introducing the high toxicity imparted by the significantly high solid content of composition C. The response to sutures alone was used as a control, and

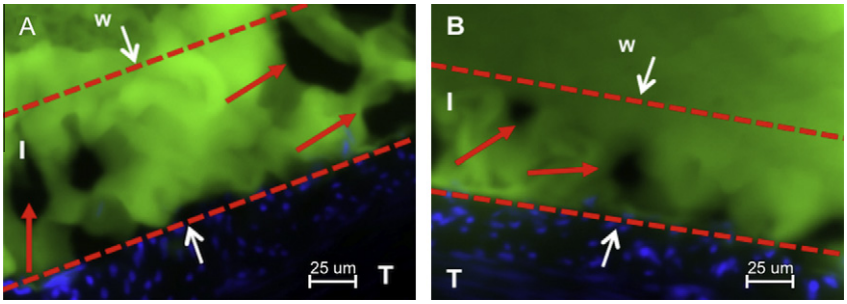

Fig. 4. Morphology of the interfacial region between the two material formulations and excised rat small intestinal tissues using quantitative fluorescence microscopy. (A) Composition A with 50% oxidation, D10-50-8.75 P8-10-25 (relative intensity 19.3 ± 2.3); (B) composition D with 20% oxidation, D10-20-23 P8-10-25 (relative intensity 14.1 ± 1.2). Three distinct regions are shown: T, tissue; I, interfacial region between the tissue and the adhesive material; B, bulk adhesive material.

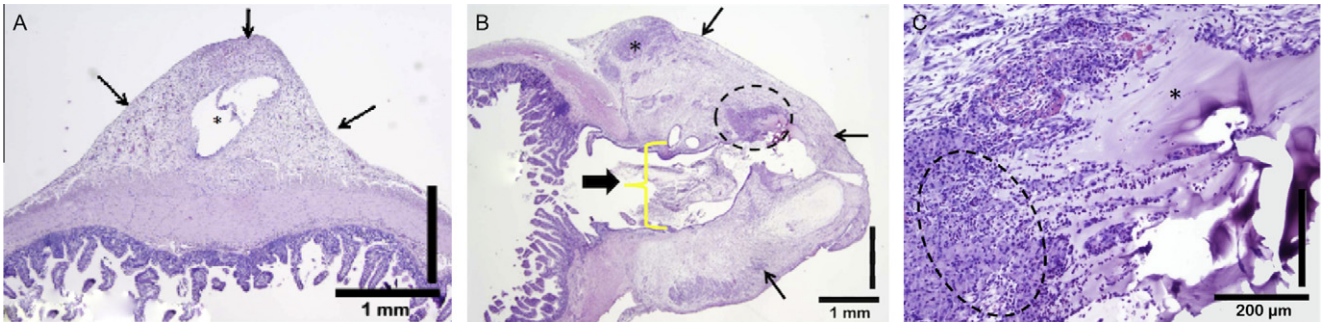

Fig. 5. Hematoxylin and eosin staining of rabbit small intestinal tissue after 15 days of adhesive application with (A) composition A, D10-50-8.75 P8-10-25 and (B) composition B, D10-50-14 P8-10-25. Scale bar is 1 mm. (C) Magnification of the dashed area seen in (B). Scale bar 200 μm.

scorings of the immunohistological sections were compared (see Section 2).

The overall inflammatory response did not extend beyond the area of healing, nor did it involve heterophilic infiltrates with necrosis. Composition A (8.75 wt.% dextran aldehyde) imparted a negligible tissue response (score 0), similar to that of sutures alone (Fig. 5A). In contrast, composition B (14 wt.% dextran aldehyde) induced a higher inflammatory score (score 2), including granoulomatous inflammation with lower re-epithelialization (Fig. 5B) and inflammatory infiltrates, including histocytes and macrophages (Fig. 5C). These results reiterate the need to optimize adhesive materials in the context of both improved mechanical performance and tolerable in vivo response.

4. Discussion

It is increasingly appreciated that each tissue and application environment presents unique targets and demands on biomaterials and thus the principles and approaches to tissue-specific and application-specific materials design are of growing interest. For example, the pH, surface texture, tissue composition and structure of the liver, lung, gastrointestinal tract and heart tissues are all significantly different. It is, therefore, plausible that similar materials will interact differently with each of these tissue types, as we have observed previously for PEG:dextran cross-linked hydrogels [13]. The present study demonstrates the ability to quantify the adhesion of a material to a target tissue by assaying the reaction sites on the tissue and material for a pair components, requiring only small sample volumes compatible with higher throughput methods.

4.1. Effects of PEG:dextran polymer design at the molecular scale

As material aldehydes react with tissue amines, one can determine the potential binding force an aldehyde-based material would exhibit based on the number of free aldehyde groups and available tissue amines. Here, AFM probes were functionalized with amine groups to represent the tissue surface functionality. The unbinding force of the PEG:dextran adhesives was used to establish the binding or interaction potential of these adhesives to tissues exhibiting a range of amine-reactive groups. As would be required of such a small scale materials optimization approach, the effects of adhesive composition observed by this molecular scale method were correlated with those determined from macroscopic mechanical challenges under uniaxial and multiaxial ex vivo loading of the adhesive–tissue interface (see Section 3.2).

4.2. Effect of material composition on failure resistance and modes

We found that increasing the solid content of PEG:dextran adhesive hydrogels was an efficient means to increase adhesion across all experimental length scales and loading challenges. Compositions A–C exhibited increased resistance to mechanical failure of the sealed interface, whether considering the nanoNewton scale unbinding force of AFM force spectroscopy (Fig. 1), the Newton scale failure force of tissue–adhesive–tissue constructs under normal loading (Fig. 2) or the Pascal scale burst pressures of sealed puncture wounds under triaxial loading (Fig. 3). The degree of cross-linking depends in part on the solid volume fraction within such hydrogels, consistent with the strong correlation between the molecular scale unbinding force and the macro scale adhesive force under uniaxial loading of the interface for the series of compositions A–C (Fig. 2B).

We also varied the percentage dextran oxidation to alter the aldehyde density within polymers with an otherwise comparable number of aldehyde groups (compositions A and D). We found that the resistance to macroscopic adhesive failure depended not only on the number of aldehyde groups per polymer chain within the hydrogel (A vs. D), but also on the loading form. This can be understood by the differences in the extent of cross-linking between these formulations, on the one hand, and the extent of reaction between dextran aldehydes and tissue amines, on the other. While a higher degree of oxidation resulted in more reactive groups per chain, facilitating the interaction between aldehydes and amines and increasing the extent of cross-linking, at the expense of tissue–material bond formation (Fig. 4). It is plausible that aldehydes in composition A formed bonds with PEG amines more efficiently than with tissue amines and thus better resisted uniaxial failure where cohesive failure was observed. In contrast, aldehydes in composition D were distributed in a way that facilitated better reaction with tissue amines rather than PEG amines, thus resisting macroscopic failure under triaxial loading, where failure was seen at the tissue–material interface. However, as noted above, the higher degradation rate of the more loosely cross-linked network of adhesive composition D decreased the utility of this material in vivo. When the objective of adhesive material optimization is to understand the most efficient means to increase failure strength, multiple means of mechanical characterization provide this capacity. Here, by comparing the failure modes (adhesive vs. cohesive) and effects of composition (number vs. density of aldehyde groups) among three mechanical characterization approaches we inferred the extent to which dextran aldehydes react with PEG amines (within the adhesive material) vs. tissue amines (at the tissue–adhesive interface).

4.3. Further consideration of application-relevant measurements of "adhesion strength"

The resistance to adhesive failure, if measured as the stress (or even load) required to disrupt the integrity of the material interface, is often loosely termed 'adhesion strength'. More accurately, this quantity is a loss of adhesion between two surfaces and can arise as a result of loss of the interfacial strength conferred by

adhesion or intra-material interactions determined by cohesion. The adhesion strength of materials to biological tissues is commonly characterized by tensile or peel tests [22,23]. Measurement of the adhesion of specific chemical groups to specific surfaces is an emerging approach [24,25] that can provide additional insight. Lee et al. reported the adhesion strength of single DOPA residues to a wet metal oxide surface via AFM force spectroscopy [11], quantified by estimating the magnitude of bond dissociation energy. While previous measures of material–tissue interaction have focused on potential chemical interactions at the multi-molecular scale or the resistance to adhesive failure on the macro scale, we have now compared these two length scales and measures of adhesive material performance directly. Additionally, we have noted that the predictive capacity of macroscopic ex vivo experiments requires that this mechanical loading is designed within the context of in vivo application loading and state.

Although there are several distinct types of macro scale mechanical tests to quantify the resistance to adhesive failure between surfaces, the stress states exerted on the material and the interface during tensile tests, peel tests or burst pressure tests are different. As a result, even the trends in failure resistance with adhesive material composition can depend on mechanical loading. For example, Ono et al. demonstrated that inverse trends can result when materials are tested in tensile or burst mode [26].

AFM-enabled force spectroscopy and macro scale tissue–adhesive–tissue rupture experiments approximated a uniaxial tensile stress state at the interface and, hence, these failure loads were well correlated (Fig. 1B vs. 2C). In contrast, the tissue samples in the burst pressure experiment were under a more complex, multiaxial stress state (Fig. 3B). With this in mind, it is not surprising that composition D, despite displaying decreased cohesive strength compared with composition A (Fig. 2C), presented a higher macroscopic burst pressure under the triaxial stress state most representative of perfused organs, such as the small intestine (Fig. 3C). Our experiments demonstrate that the distribution of aldehyde groups along the exposed chains plays a key role in adhesion to these tissues for the practical application of interest, sealing of open serosal wounds of the small intestine subjected to perfusion pressure. Thus, adhesive materials for in vivo use require that macro scale experiments should reflect the mechanical loading states anticipated for wound sealing applications in vivo.

4.4. Targeting adhesive polymers for specific tissues and applications

Our in vivo studies revealed increasing cytotoxicity of the PEG:dextran hydrogels with increasing solid content. Both the adhesion score and the inflammatory response were higher in composition B than in composition A. In fact, composition A showed a tissue response comparable with that of sutures alone, demonstrating that lowering the adhesive aldehyde content reduced the adverse biocompatibility of the sealant. Although molecular scale and macro scale measures of adhesion failure resistance can facilitate the design of new adhesive polymer families, biocompatibility remains an important component of adhesive material optimization. Even in these adhesives, comprising biocompatible constituents, higher adhesion and failure strength ex vivo could correlate with increasingly adverse tissue reactions in vivo. The requirements of materials rise as applications increase in complexity. Adhesive sealing of duodenal wounds, for example, requires a composition exhibiting a high burst pressure (to prevent leakage of gut content after internal surgery), a low degradation rate and a minimal inflammatory response. The family of PEG:dextrans under consideration demonstrate that: (1) an increased aldehyde content correlates with the adhesion strength for all modes of evaluation, but also an increased inflammatory response; (2) a lower aldehyde density correlates with an increased burst pressure failure and improved interfacial morphology of the serosal wound, but also increased degradation rates in vivo; (3) all adhesive materials considered exhibited super-physiological interfacial failure strengths under the anticipated in vivo mechanical loading challenge. Thus, for the specific application of interest in vivo, sealing of open serosal wounds of the small intestine, composition A, which comprises 10 kDa 8.75 wt.% dextran aldehyde with 50% oxidation (D10-50-8.75 P8-10-25) provides an optimal balance of mechanical performance, seal stability over time and biological tolerance.

5. Conclusions

Polymer materials designed as adhesives for biological applications require optimization of interfacial failure resistance, degradation rates and biocompatibility. When the interfacial chemical reactions between the adhesive and tissue target are well defined, such as in the case of PEG:dextran adhesives and soft tissue organs such as the duodenum, mechanical characterization of this adhesion potential can be quantified across length scales and mechanical conditions. AFM-enabled force spectroscopy offers the opportunity to define a specific binding potential for a given material and a given target tissue and is predictive of the macro scale resistance to adhesive failure modes of the adhesive sealants and tissues considered herein. Ultimately, the macroscopic characterization of failure should consider mechanical loading profiles relevant to the tissue/organ application of interest. Finally, while this resistance to failure of an adhesively sealed tissue interface is an important factor in the development of materials for biological sealants, in vivo experiments are still required to optimize the "adhesion strength" in the context of sufficient biocompatibility.

Acknowledgements

Krystyn Van Vliet acknowledges a NSF Career Award and Adam Zeiger a NDSEG Fellowship and ERE National Institutes of Health grant (GM 49039).

Appendix A. Supplementary data

Supplementary data associated with this article can be found, in the online version, at doi:10.1016/j.actbio.2010.07.008.

Appendix B. Figures with essential colour discrimination

Certain figures in this article, particularly Figures 1–5, are difficult to interpret in black and white. The full colour images can be found in the online version, at doi:10.1016/j.actbio.2010.07.008.

References

[1] Hilgert LA, Lopes GC, Araujo E, Baratieri LN. Adhesive procedures in daily practice: essential aspects. Compend Contin Educ Dent 2008;29(4):208–15. quiz 16, 18.
[2] Berdahl JP, Johnson CS, Proia AD, Grinstaff MW, Kim T. Comparison of sutures and dendritic polymer adhesives for corneal laceration repair in an in vivo chicken model. Arch Ophthalmol 2009;127(4):442–7.
[3] Saunders MM, Baxter ZC, Abou-Elella A, Kunselman AR, Trussell JC. BioGlue and Dermabond save time, leak less, and are not mechanically inferior to two-layer and modified one-layer vasovasostomy. Fertil Steril 2009;91(2):560–5.
[4] Martens TP, Godier AF, Parks JJ, Wan LQ, Koeckert MS, Eng GM, et al. Percutaneous cell delivery into the heart using hydrogels polymerizing in situ. Cell Transpl 2009;18(3):297–304.
[5] Papatheofanis FJ, Ray RD. Experimental use of adhesives in the repair of transverse fractures of the rat and rabbit. Biomater Med Devices Artif Organs 1983;10(4):247–65.
[6] Tireli E, Ugurlucan M. EComment: fibrin glue reinforced Teflon felt sandwich for the prevention of anastomotic leak in replacement of ascending aorta for acute aortic dissection. Interact Cardiovasc Thoracic Surg 2009;9(2):212–3.
[7] Hall RC, Logan AJ, Wells AP. Comparison of fibrin glue with sutures for pterygium excision surgery with conjunctival autografts. Clin Exp Ophthalmol 2009;37(6):584–9.

[8] Maniwa T, Kaneda H, Saito Y. Management of a complicated pulmonary fistula caused by lung cancer using a fibrin glue-soaked polyglycolic acid sheet covered with an intercostal muscle flap. Interact Cardiovasc Thoracic Surg 2009;8(6):697–8.
[9] Vinatier C, Gauthier O, Masson M, Malard O, Moreau A, Fellah BH, et al. Nasal chondrocytes and fibrin sealant for cartilage tissue engineering. J Biomed Mater Res 2009;89(1):176–85.
[10] Lee H, Lee BP, Messersmith PB. A reversible wet/dry adhesive inspired by mussels and geckos. Nature 2007;448(7151):338–41.
[11] Lee H, Scherer NF, Messersmith PB. Single-molecule mechanics of mussel adhesion. Proc Natl Acad Sci USA 2006;103(35):12999–3003.
[12] Mahdavi A, Ferreira L, Sundback C, Nichol JW, Chan EP, Carter DJ, et al. A biodegradable and biocompatible gecko-inspired tissue adhesive. Proc Natl Acad Sci USA 2008;105(7):2307–12.
[13] Artzi N, Shazly T, Baker AB, Bon A, Edelman ER. Aldehyde–amine chemistry enables modulated biosealants with tissue-specific adhesion. Adv Mater 2009;21(32):3399–403.
[14] Shazly TM, Artzi N, Boehning F, Edelman ER. Viscoelastic adhesive mechanics of aldehyde-mediated soft tissue sealants. Biomaterials 2008;29(35): 4584–91.
[15] Artzi N, Shazly T, Crespo C, Ramos AB, Chenault HK, Edelman ER. Characterization of star adhesive sealants based on PEG/dextran hydrogels. Macromol Biosci 2009;9(8):754–65.
[16] Cleveland JP, Manne S, Bocek D, Hansma PK. A nondestructive method for determining the spring constant of cantilevers for scanning force microscopy. Rev Sci Instrum 1993;64(2):403–5.
[17] Lee S, Mandic J, Van Vliet KJ. Chemomechanical mapping of ligand-receptor binding kinetics on cells. Proc Natl Acad Sci USA 2007;104(23):9609–14.
[18] Van Vliet KJ, Bao G, Suresh S. The biomechanics toolbox: experimental approaches for living cells and biomolecules. Acta Mater 2003;51: 5881–905.
[19] Azadani AN, Matthews PB, Ge L, Shen Y, Jhun CS, Guy TS, et al. Mechanical properties of surgical glues used in aortic root replacement. Ann Thoracic Surg 2009;87(4):1154–60.
[20] Rickett T, Li J, Patel M, Sun W, Leung G, Shi R. Ethyl-cyanoacrylate is acutely nontoxic and provides sufficient bond strength for anastomosis of peripheral nerves. J Biomed Mater Res 2009;90(3):750–4.
[21] Kalloo AN, Pasricha PJ. Effect of gastric distension and duodenal fat infusion on biliary sphincter of Oddi motility in healthy volunteers. Dig Dis Sci 1995;40(4):745–8.
[22] Nussinovitch A, Gal A, Padula C, Santi P. Physical characterization of a new skin bioadhesive film. AAPS Pharm Sci Tech 2008;9(2):458–63.
[23] Wilson DJ, Chenery DH, Bowring HK, Wilson K, Turner R, Maughan J, et al. Physical and biological properties of a novel siloxane adhesive for soft tissue applications. J Biomater Sci 2005;16(4):449–72.
[24] Pirzer T, Geisler M, Scheibel T, Hugel T. Single molecule force measurements delineate salt, pH and surface effects on biopolymer adhesion. Phys Biol 2009;6(2):025004.
[25] Sonnenberg L, Parvole J, Kuhner F, Billon L, Gaub HE. Choose sides: differential polymer adhesion. Langmuir 2007;23(12):6660–6.
[26] Ono K, Saito Y, Yura H, Ishikawa K, Kurita A, Akaike T, et al. Photocrosslinkable chitosan as a biological adhesive. J Biomed Mater Res 2000;49(2):289–95.